

# Joint scaling laws in functional and evolutionary categories in prokaryotic genomes.

Jacopo Grilli<sup>1</sup>, Bruno Bassetti<sup>1,2</sup>, Sergei Maslov<sup>3</sup>, Marco Cosentino Lagomarsino<sup>4,5,\*</sup>

**1** Dipartimento di Fisica, Università degli Studi di Milano, Milano, Italy

**2** I.N.F.N. Milano, Milano, Italy

**3** Department of Condensed Matter Physics and Materials Science, Brookhaven National Laboratory, Upton, NY 11973, United States of America

**4** Génophysique / Genomic Physics Group, UMR 7238 CNRS “Microorganism Genomics”, Paris, France

**5** Université Pierre et Marie Curie, Paris, France

\* E-mail: Marco.Cosentino-Lagomarsino@upmc.fr

## Abstract

We propose and study a duplication-innovation-loss model of genome evolution taking into account biological roles of constituent genes. In our model numbers of genes in different functional categories are coupled to each other. For example, an increase in the number of metabolic enzymes in a genome is usually accompanied by addition of new transcription factors regulating these enzymes. Such coupling can be thought of as a proportional “recipe” for genome composition of the type “a spoonful of sugar for each egg yolk”. The model jointly reproduces two known empirical scaling laws: the scale-free distribution of family sizes and the nonlinear scaling of the number of genes in certain functional categories with genome size. In addition, it allows us to derive a novel relation between the exponents characterizing these two scaling laws. This mathematical property of our model was subsequently confirmed in real-life prokaryotic genomes. To further support the assumptions of our model we present an empirical evidence of correlations between functional repertoires of prokaryotic genomes. The overall pattern of these correlations remains mostly unchanged when large and small genomes are analyzed separately. This hints at universality of biological mechanisms shaping up prokaryotic genomes irrespective of their size.

## Introduction

Protein-coding genes in genomes can be classified in both functional categories (e.g. transcription factors or metabolic enzymes) as well as “evolutionary categories” or families of homologous genes<sup>1</sup>. Functional categories are routinely composed of a large number of evolutionary ones. This distinction is illustrated in Fig. 1 where genes are characterized by both shape (functional category) and color (homology class) with each shape represented by multiple colors. Understanding the principles connecting these separate classifications of genomic material is an important and necessary step in order to shed light on the mechanisms through which genomes evolve.

Studies of fully sequenced genomes revealed that their functional and evolutionary composition is governed by simple quantitative laws [1,2]. In particular, for prokaryotes the number of genes in individual functional categories was shown to scale as a power law of the total number of genes in the genome [2]. Depending on the functional category the exponent of this scaling law varies from 0 (for fixed sets of housekeeping genes) to 1 (for metabolic enzymes) and all the way up to 2 (for transcription factors and kinases) [2,3]. Furthermore, the distribution of sizes of gene families (called “evolutionary categories” in our title) has a scale-free distribution with the exponent inversely correlated with the genome size [1,4,5]. The overall number of gene (or domain) families represented by at least one member exhibits a slower-than-linear scaling with the total number of genes in a genome [6,7].

<sup>1</sup>To avoid confusion, in the following we will reserve the term “category” to functional annotations, and we will use the term “family” as a generic indication of homology classes (or domain families/superfamilies in domain data, see Methods).

These empirical laws allow one to construct models that explore different design principles, or more prosaically the recipes by which genomes are built from elementary functional and evolutionary ingredients. In this study we introduce the first model to simultaneously reproduce all of the empirically observed scaling laws for both functional and evolutionary categories.

Several theoretical models have been previously proposed to explain the power-law distribution of family sizes [5, 8–11]. Most of these models are of duplication-innovation-loss type. We recently formulated a related model that in addition to family size distribution also explains and successfully fits the scaling of the number of distinct gene families represented in a genome as a function of genome size [6, 12].

On another front, the toolbox model of evolution of metabolic networks and their regulation recently proposed by one of us [13] offered an explanation for the quadratic scaling between the number of transcription factors and the total number of genes in prokaryotes. In this model, metabolic and regulatory networks of prokaryotes are shaped by addition of co-regulated metabolic pathways. The number of added enzymes systematically decreases with the proportion to which the organism has already explored the universe of available metabolic reactions, and thus, indirectly, with the size of its genome. For the purposes of the present study, a key ingredient of the toolbox model is that events adding or deleting genes in multiple functional categories (in this case metabolic enzymes and transcription factors regulating metabolic pathways) are tightly correlated with each other.

The concept of coordinated expansion or contraction of functional categories can be easily extended beyond enzymes and their regulators. Specific biological details of how categories are correlated with each other determine the scaling exponents relating their genome fractions to each other and genome size. One should note that this explanation of scaling of functional categories is conceptually different from that based on “evolutionary potentials” proposed in Ref. [3]. Evolutionary potentials quantify the intrinsic growth rates of individual categories and as such they are a priori uncoupled from growth or decline in other functional categories. At the same time, coordinated expansion of multiple functional categories caused e.g. by evolutionary optimization and/or constraints can be in fact the underlying determinant of their effective evolutionary potentials.

This study brings together the basic ingredients of duplication-innovation-loss models [6, 12] and coordinated growth of functional categories dictated by the toolbox model [13]. The resulting combination allows us to study the interplay between the scaling of evolutionary and functional categories. In particular, we mathematically derive a relation between the exponents characterizing these two scaling laws. It predicts that functional categories that grow faster-than-linearly with genome size are characterized by steeper-than-average family size distributions. This prediction of our model is subsequently verified by our analysis of functional and evolutionary scaling in empirical data on sequenced prokaryotic genomes.

## Model

The model represents a genome as a list of genes, which is partitioned in homology families and functional categories. Genome evolution is modeled as a stochastic process where the elementary moves can be any of two types: (i) a “family expansion” or “duplication” move in which a new domain is placed in an evolutionary category (family of homologous domains) already present in the genome or (ii) an “innovation” move in which a new family with just one domain appears in a genome (e.g. by the virtue of horizontal gene transfer).

We would like to emphasize that by labeling the family expansion move as duplication we simply follow the tradition established in duplication-innovation-loss models. In reality this move can come either by the virtue of gene duplication or by horizontal gene transfer which is the dominant evolutionary mechanism in bacteria. The overall family size in all genomes is generating an effective “preferential attachment” for HGT events (see Refs. [3, 14] and open comments by referees therein).

Although genes are natural objects of this kind of description, it is not simple to use genes as central units in the analysis of empirical data, mainly due to the fact that gene dynamics is complex and may

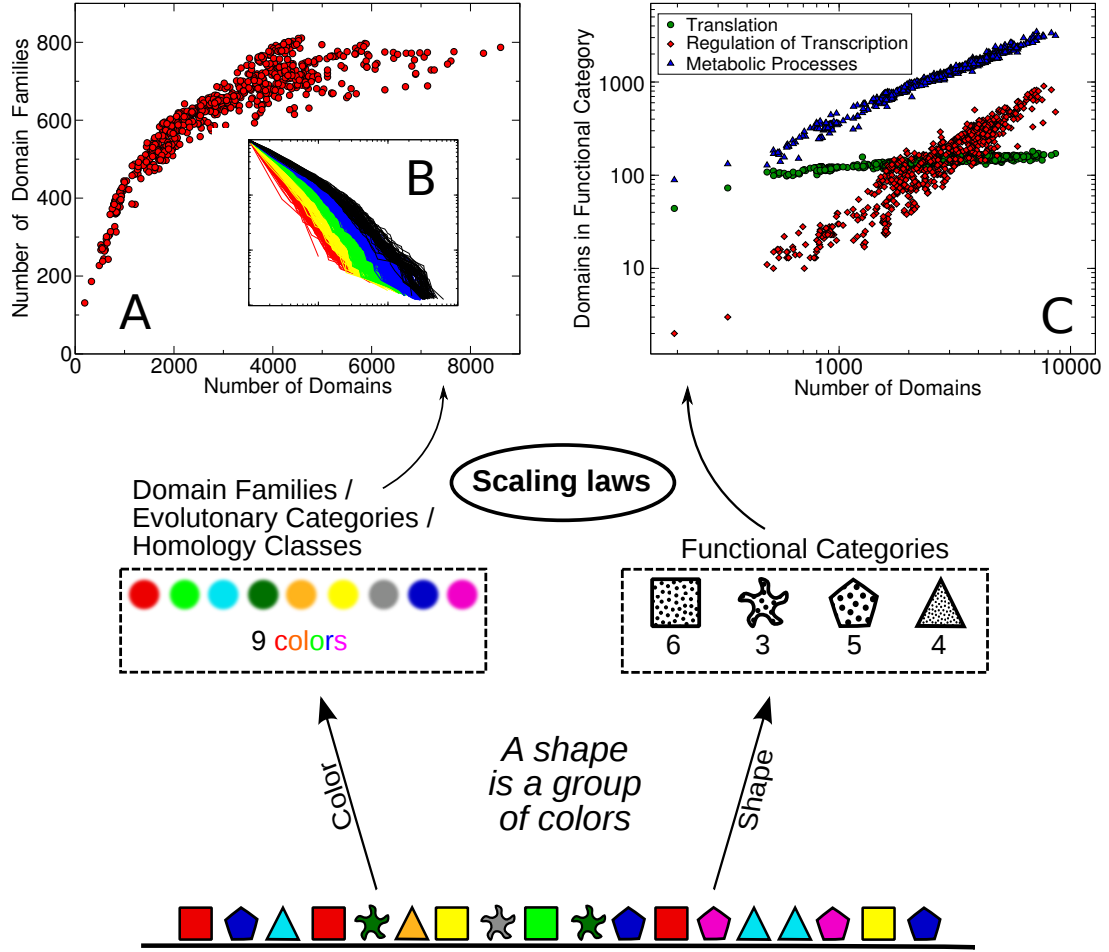


**Figure 1. Scaling laws in partitioning of genomes into families of homologous genes (colors) and functional categories (shapes).** (A) The number of unique evolutionary categories (domain families) (y-axis) scales sub-linearly with the genome size (x-axis) (B) Domain family population cumulative histograms (see Figure 3). (C) The number of transcriptional regulators (red), metabolic enzymes (blue), and housekeeping genes responsible for translation (green) plotted as a function of the genome size measured in the total number of domains. Symbols in the plots are empirical data for protein domains in 753 fully sequenced bacterial genomes.

contain events of gene fusion, splitting and internal rearrangements. Thus, as in some previous analyses, we will compare the models with data on protein domains [3,6], which have the important property that they cannot be split into smaller units [15]. Domains are modular building blocks of proteins and it has been argued that they effectively work as the natural atomic elements in genome evolution [4]. Concerning the scaling laws, domains appear to have the same qualitative behaviour as genes. Throughout the paper, we will be comparing the models with data on 753 bacteria from the SUPERFAMILY database [16]. The models will be formulated for abstract atomic elements that could be genes or domains, and possible relevant issues when dealing empirically with genes will be addressed in the discussion. In describing the models we will generally refer to these units as genes.

## Standard Chinese Restaurant Process

The starting point is a duplication-innovation process for the homology families that reproduces qualitatively the empirical scaling laws [6]. This process (known in mathematical literature as “Chinese Restaurant Process” or CRP [17]) defines a growth dynamics for the partitioning of a set of elements (genes or domains) based on two basic growth moves. Traditionally the CRP model is defined by two parameters  $\alpha$  and  $\theta$  constrained by  $0 \leq \alpha \leq 1$  and  $\theta > -\alpha$ . The moves are quantified and defined by two probabilities  $p_O$  and  $p_N$  of duplication and innovation respectively.

- The duplication probability  $p_O^i$  of a domain family  $i$  is proportional to the number of family members  $n_i$  currently in the genome offset by  $\alpha$ :  $p_O^i \sim n_i - \alpha$  (see Table 1).
- The innovation probability  $p_N$  is the probability of adding a new domain family with one member. It corresponds to a new domain family appearing in a genome by *de novo* evolution or horizontal gene transfer. The CRP model assumes  $p_N \sim \alpha f + \theta$ , where  $f$  is the total number of domain families present in the genome.

The normalization condition  $p_N + \sum_i p_O^i = 1$  determines the pre-factor in both equations to be  $1/(n + \theta)$ . A gene loss move does not seem to be essential for the basic qualitative results. Indeed, if stochastic (uniform) gene loss is incorporated into the model it results only in renormalization of parameters  $p_O$  and  $p_N$  [12].

We explore the model by direct simulation and by solving continuous “mean-field” equations [6,12] that describe the mean behaviour of the number of homology families and functional categories, and the statistics of the population of families and categories.

## CRP model incorporating functional categories.

In order to introduce functional categories into the CRP, one has to specify  $p_O$  and  $p_N$  for different categories. We first assume that the probability of introducing a gene of a specific functional category by the innovation move is independent of genome size. This assumption implies that the number of homology families of a given category scales linearly in the total number of families, and is roughly justified empirically for some functional categories by domain data (see Supplementary Figure S1 and S2). Equivalently,  $p_N^c = \chi_c p_N$ , where  $\chi_c$  is the probability of introducing a new family of the category  $c$ .

Under this assumption, the mean-field equation describing the growth of a family of homologous domains (evolutionary category) is

$$C(n) \partial_n n_i = \sum_{j=1}^f (\delta_{ij} + a_{ij})(n_j - \alpha). \quad (1)$$

Here the genome size  $n$  is used instead of time and averages over multiple realizations of a process are implied. The novel ingredient of the model - coordinated growth of functional categories - is encoded

in the coefficients  $a_{ij}$  responsible for correlated duplications between evolutionary families  $i$  and  $j$ . We assume  $a_{ij}$  to depend only on functional roles of families  $i$  and  $j$ . The equation describing the growth of  $f$  - the number of distinct families in a genome is the same as in a standard CRP model.

$$C(n)\partial_n f = (\alpha f + \theta) . \quad (2)$$

The function  $C(n)$ , which sets a natural time scale for the process, is determined by the normalization condition  $\partial_n n = 1$ , i.e.  $\sum_i \partial_n n_i + \partial_n f = 1$ .

For the specific case of categories of transcription factors regulating metabolic processes (TFs) and their metabolic target genes, the necessity of a correlated move can be argued along the lines of Ref. [13]. A set of new targets has to be added to incorporate a new metabolic function. This set corresponds to a branch of the metabolic network connected to the core metabolism, and a newly added branch is controlled by one transcription factor. Since the length of the branch becomes smaller with increasing size of the organismal metabolic network (compared to a metabolic “universe”), on average, increasingly more TFs per target will be needed in order to control newly incorporated branches. More generally, functional, genetic and epistatic interactions can create the correlated growth of different functional categories of genes. In the discussion section we provide the empirical evidence of statistically significant correlations between various functional categories.

Following the recipe outlined in Ref. [13] and consider a simplified version of our model involving only two functional categories: 1) *TF* - transcription factors controlling metabolic processes; 2) *met* - metabolic enzymes they regulated. The toolbox model (or more generally any model leading to quadratic scaling) dictates that changes in  $n_{TF}$  and  $n_{met}$  must be coordinated with correlation coefficients  $a_{ij}$  given by

$$\begin{aligned} a_{ij} &= \frac{n_j}{n_{met}}, \\ a_{ji} &= 0. \end{aligned}$$

Here  $i$  denotes any gene family from functional category *TF* and  $j$  - from the functional category *met*. Integration of Eqs. 1 and summation over all domain families from functional categories *TF* and *met* then gives  $dn_{TF}/dn_{met} = 2(n_{TF} - \alpha)/(n_{met} - \alpha) \simeq 2n_{TF}/n_{met}$  or finally the desired quadratic scaling  $n_{TF} \sim n_{met}^2$ .

We also considered, as a variant of our model, an effective model where correlations between functional categories are absent, but instead members of a given functional category are added at a category-dependent intrinsic rate as prescribed by “evolutionary potentials” of Molina and van Nimwegen. The results of these simulations will be discussed later on in the manuscript and compared to our main “correlated duplication” model. (see Discussion and Supplementary Text S1).

## Results

### Correlated growth model captures the combined scaling laws

Numerical simulation and mean-field analytical solutions of the correlated growth model reproduce very well both the empirical behavior of the TFs scaling law and the statistics for evolutionary domain families (Figure 2). This agreement is universal, in the sense that the same three parameters are sufficient to predict family/category numbers and populations for all genomes in the dataset. Moreover, the comparison does not rely on the adjustment on any free or hidden parameter. It is also worthwhile noting that, while the input of this model, the toolbox model, is built to give a power-law scaling exponent of two for transcription factors (which is reproduced by the mean-field approach), at the relevant genome sizes the model automatically reproduces the *correct* empirical exponent (about 1.6 in the SUPERFAMILY data). Note that in this model TFs can duplicate both spontaneously (uncorrelated move) and following spontaneous duplication of targets (correlated move), corresponding to the terms  $\delta_{ij}$  and  $a_{ij}$  in equation 1.

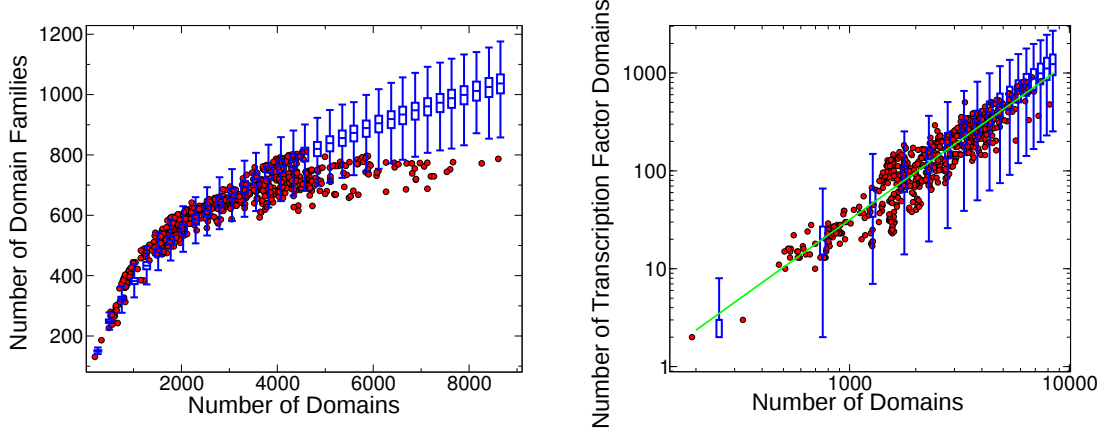


**Figure 2. Comparison between 1000 realizations of the correlated duplication model variant** at  $\alpha = 0.3$  and  $\theta = 140$  (blue boxplot) with empirical data (red). The left panel is a plot of the number of domain families versus genome size. The fact that the number of families does not saturate is a property of the standard duplication-innovation model (see [6] for a complete discussion). The right panel plots the number of TF domains vs. the total number of domains, showing that the scaling of the transcription functional category is well reproduced. The green line represents the best fit of empirical data (exponent 1.6)

The extension of the model to more than two categories requires to know the laws through which families of different categories are correlated each other. Supplementary Figure S3 compares the results obtained by a correlated duplication model formulated with three categories (TFs, met, others).

### Prediction of the exponents of the family-population histogram restricted to single functional categories.

While the agreement between model and data shows that the scaling of functional and evolutionary categories can be understood jointly, it does not provide by itself any substantially new information about how the two partitionings interact. Further insight can be obtained considering the population of evolutionary families belonging to a specific functional category. In general, the population of domain families of a genome follows a near power law distribution whose slope depends on genome size (Figure 3). The mean number  $f(d, n)$  of domain families having  $d$  members at large genome size  $n$  is well described by the slope  $1/d^{1+\beta}$  (see Figure 3), and thus the cumulative histogram by  $Q(d, n) \sim 1/d^\beta$ , where the fitted exponent  $\beta$  typically lies between 0 and 1. The standard CRP predicts this behavior [6, 12]. The model described here allows to consider the same histograms restricted to specific functional categories (Figure 3 and Figures 5).

A mean-field calculation (see Supplementary Text S2) based on the model variant with correlated duplication predicts that the different trend of domain population histograms for transcription-factor families scales as  $f(d, n)_{TF} \sim 1/d^{1+\frac{\beta}{2}}$  (see Figure 4). Thus, the ratio between the exponent of the cumulative histogram of all families and the exponent of the cumulative histogram restricted to families belonging to the transcription factor category is predicted to be equal to the mean-field exponent for the scaling of the functional category. More in general, the model predicts that each time the per-family duplication probability for a functional category takes the form  $p_O^c \simeq \zeta_c N_c$ , the coefficient  $\zeta_c$  will appear in the equation for  $P(d)_c$  modifying the exponent such as  $\beta_c = \beta/\zeta_c$  (Supplementary Text S2). In other words, a precise quantitative relationship must exist between the scaling exponent of a category and the

**Table 1. Basic Mathematical Quantities and notation**

Quantity	Meaning
$\alpha, \theta$	CRP model parameters
$n$	Genome size quantified by its total number of domains
$n_i$	Number of domains in the family $i$
$n_c$	Number of domains in the functional category $c$
$f(n)$	Number of families in a genome of size $n$
$f_c(n)$	Number of families in a genome of size $n$ belonging to the functional category $c$
$f(d, n)$	Number of families with exactly $d$ members in a genome of size $n$
$f_c(d, n)$	Number of families belonging to the functional category $c$ with exactly $d$ members in a genome of size $n$
$\beta$	Exponent of the family-population histogram
$\beta_c$	Exponent of the family-population histogram restricted to category $c$
$\chi_c$	Probability to introduce a new family of the category $c$ (empirically quantified by the slope of $f_c$ vs. $f$ )
$\zeta_c$	Exponent of the scaling of the size of functional category $c$ vs. genome size $n$

**Table 2. Prediction of the exponent of the family-population histograms restricted to singular functional category**

Genome	Size	Empirical Ratio	Mean-field prediction	Empirical Scaling
Sorangium cellulosum	8610	$1.72 \pm 0.1$	2.0	1.6
Burkholderia xenovorans	8264	$1.63 \pm 0.08$	2.0	1.6
Burkholderia	7666	$1.54 \pm 0.13$	2.0	1.6
Solibacter usitatus	7605	$1.46 \pm 0.05$	2.0	1.6
Bradyrhizobium japonicum	7536	$1.59 \pm 0.11$	2.0	1.6

Comparison between expected and observed ratio of the exponent of the cumulative histogram of all families and the exponent of the cumulative histogram of transcription-factor families ( Figure 5 ), for the five largest bacteria in the SUPERFAMILY database. The ratio can be compared with the mean-field prediction of 2, or directly with the empirical exponent of the transcription factor functional category (1.6).

slope of the family population histogram restricted to the same category. Functional categories that grow faster-than-linearly with genome size will have steeper-than-average domain family size distributions. Conversely categories growing slower-than-linearly will follow a flatter-than-average slope.

Accordingly, a strongly visible trend should be expected in empirical data from families belonging to the transcription factor category, which scales with exponent 2. Indeed, the empirical population histograms for the transcription factor functional category for all the genomes in the data set have a slope that is spectacularly different from the global one (Figure 4). Quantitatively, this observation is in excellent agreement with predictions (Table 2). Direct simulations of the correlated model reproduce well both the behavior of the histograms at given size and the dependency on genome size (see Figure 3).

More in general, one can test the prediction  $\beta_c = \beta/\zeta_c$  with an empirical evaluation of many functional categories (Figure 5). The agreement of empirical data with the predicted behavior is reasonably good, keeping in mind that many functional categories are composed by few or poorly populated families, and in these cases the data might not follow a scaling law that is as clearly defined as the metabolism or the transcription factor categories.

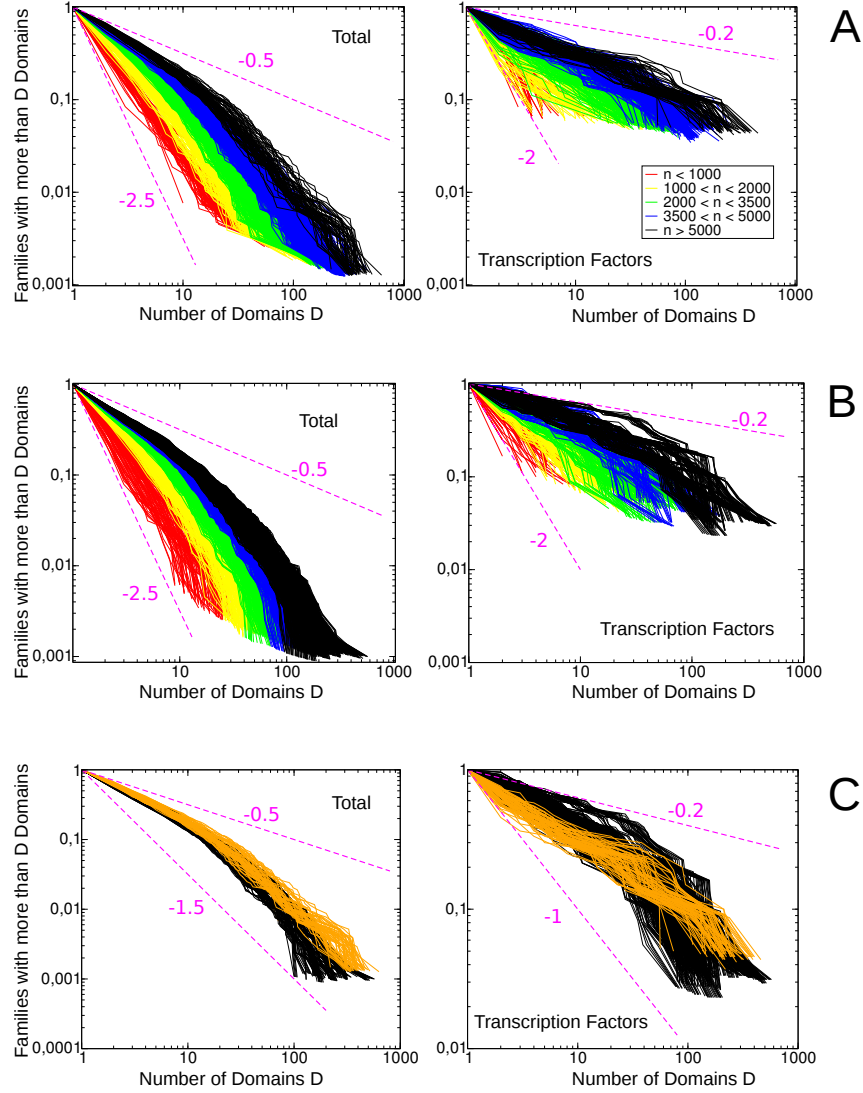


**Figure 3. Empirical data and simulations for the normalized domain family population cumulative histograms (defined as the fraction  $f(d, n)/f(n)$  of families with more than  $d$  domains).** (a) Empirical data for the 753 bacteria in the SUPERFAMILY database (each color is a set of genomes with similar sizes). Left panel: domain family population cumulative normalized histograms. Right panel: normalized cumulative histograms restricted to domain families belonging to the transcription factor functional categories. Note that the histograms slopes are different. (b) Simulations for domains family population cumulative histograms of CRP with correlated duplications run at  $\alpha = 0.3$  and  $\theta = 140$ . (a). Left panel: domain family population cumulative normalized histograms. Right panel: Transcription factor (TF) domain family population normalized cumulative histograms. (c) Comparison between simulations of the correlated duplication model variant run at  $\alpha = 0.3$  and  $\theta = 140$  (black lines) with empirical data (orange lines) for the largest genome sizes ( $5000 < n < 8500$ ). Left panel: global normalized cumulative histograms of domain family population. Right panel: normalized cumulative histograms restricted to transcription factor domain families.



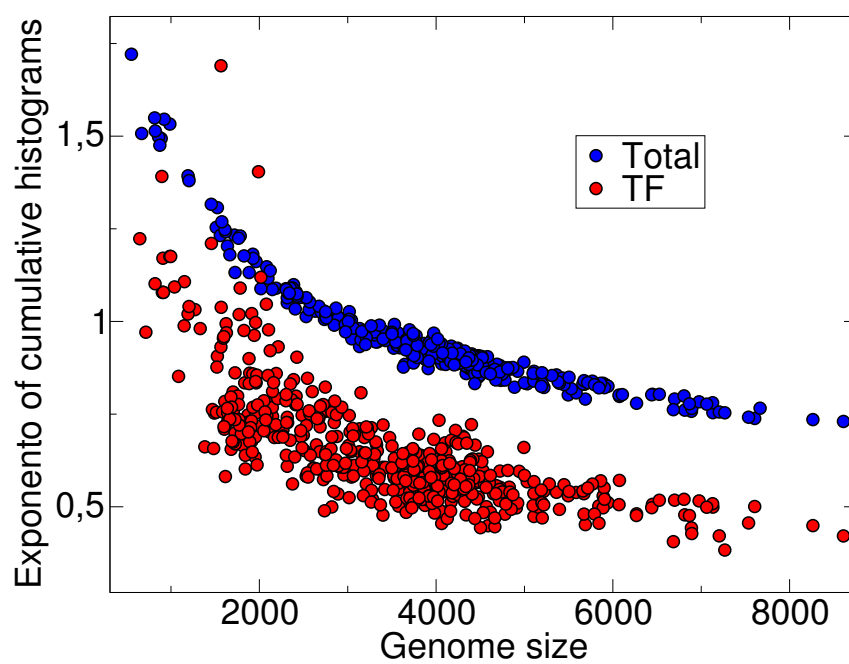


**Figure 4. Fitted exponent of domain family population cumulative histograms vs. genome size** , for the 753 bacteria in the SUPERFAMILY database for TF families (red circles) and all families (black squares), obtained by a fitting method giving a lower weight to the tail in order to keep into account the cutoffs (used in ref. [12]).

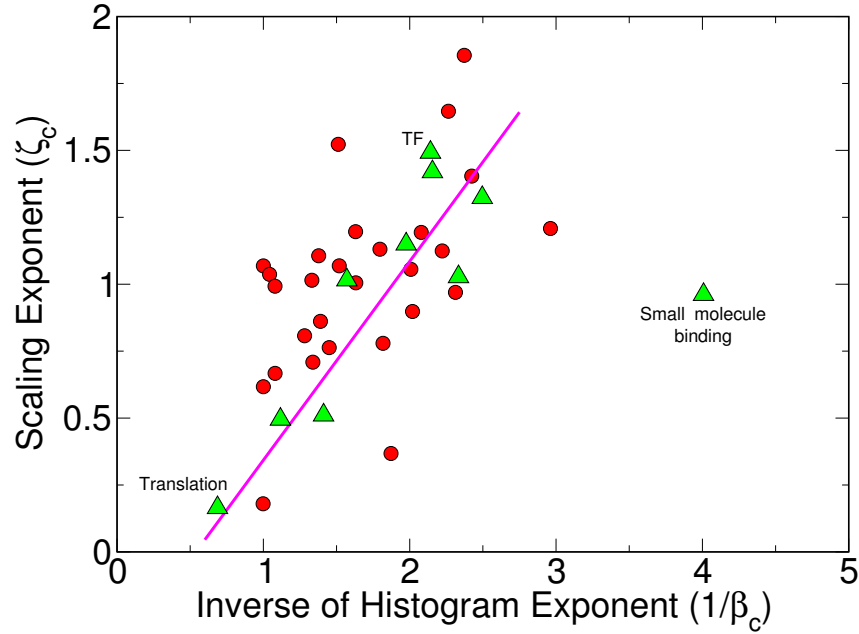


**Figure 5. Relation between histograms exponent of different categories.** Correlation between inverse histograms exponent and scaling exponent of functional categories (red points and green triangles) for 38 categories. Green triangles rerepresent the ten most populated categories, where the estimated exponents are accurate. Each data point is an average over the five largest genomes, for a given functional category. The model predicts that the correlation is linear and the slope is equal to the empirical value of  $\beta$  (magenta line, where empirical  $\beta = 0.74$  is calculated from the family population histograms of the five most populated genomes). The corresponding rank correlation coefficient is 0.55 (p-value 0.0002). The only relevant outlier is the “small molecule binding” category, which is composed of very few highly-populated domain families and is known to follow peculiar evolutionary mechanisms [18].

## Discussion

We have presented the first combined quantitative description of the partitioning of genomes in both evolutionary families and functional categories. The results show that a theoretical framework that correctly reproduces both the scaling laws for functional categories of genes/domains and the scaling laws for gene/domain families (numbers and histograms) is possible.

### Population of evolutionary families of a given functional category

The model leads to the nontrivial prediction that connects the growth exponent of a functional category to the slope of the population family histogram restricted to the same category. Specifically, the ratio between the exponent of the cumulative histogram of all families and the exponent of the cumulative histogram restricted to families belonging to a functional category is predicted to be equal to the exponent for the scaling of the functional category.

To generate this prediction, we have analyzed in detail the case of transcription factors, where the exponent of the population histogram is halved due to the quadratic scaling using mean-field calculations and simulations, and verified that it holds in general by simulations of both model variants. Empirical data on transcription factors follow this behavior remarkably well, showing population cumulative histograms of transcription factor superfamilies decaying with halved exponents compared to the global populations. The fatter tails of the TF histograms might also be related to the fact that only a few highly populated DNA-binding domain superfamilies dominate the population of TF DNA-binding domains and determine the scaling laws (Supplementary Text S4 and Supplementary Figure S4). More in general, we have also compared the behavior of domain family population histograms for all the empirical functional categories with the prediction, obtaining results that are in good agreement (Figure 5), in particular for the highly populated categories, where the fitting procedure does not . The only highly-populated category that significantly violates this general trend is small molecule binding, a category composed of very few highly-populated domain families. This category is known to follow peculiar evolutionary laws, with high mobility of domains across the metabolic network, resulting in members of the same family being scattered across different pathways and producing lineage-specific domain families, with frequent re-invention of the same function by different families [18, 19].

Technically, in order to compare with the protein domain data we rely on simplifying assumptions on the domain composition of proteins. Obviously the situation is more complex than this. We have verified in the data that the number of TF domains are linear in the number of TF genes (Supplementary Figure S5), with slope 1.09 (average number of TF domains in a TF gene). A second assumption is that the number of families belonging to a functional category is linear in the total number of families. This assumption is in accordance with data (see Supplementary Figures S1). In particular, we observed this trend for the number of transcription factor superfamilies (see Supplementary Figures S2). Charoensawan *et al* propose that the number of TF families follows a linear scaling with genome *size* [20]. If this were to be the case, the innovation dynamics of transcription factor families should be distinct from other families. In fact, if  $f_{TF}(n) \sim n$ , since the total number of families is sublinear,  $f(n) \sim n^\alpha$  in the CRP (Figure 1), then we would have  $f_{TF} f^{2-\alpha}$  that is not confirmed by the SUPERFAMILY data analyzed here (see Supplementary Figure S2).

### Correlated and absolute recipes

A strategy for defining the model, valid at least for the scaling of transcription factors, can take inspiration from the biological observation that addition of genes belonging to different categories that are related in terms of a cell task, pathway or process should follow coordinated rules [21]. This hypothesis naturally leads to the choice of correlated evolutionary moves for adding genes of different functional categories. In order to further justify this assumption, we probed directly the empirical domain data for correlated

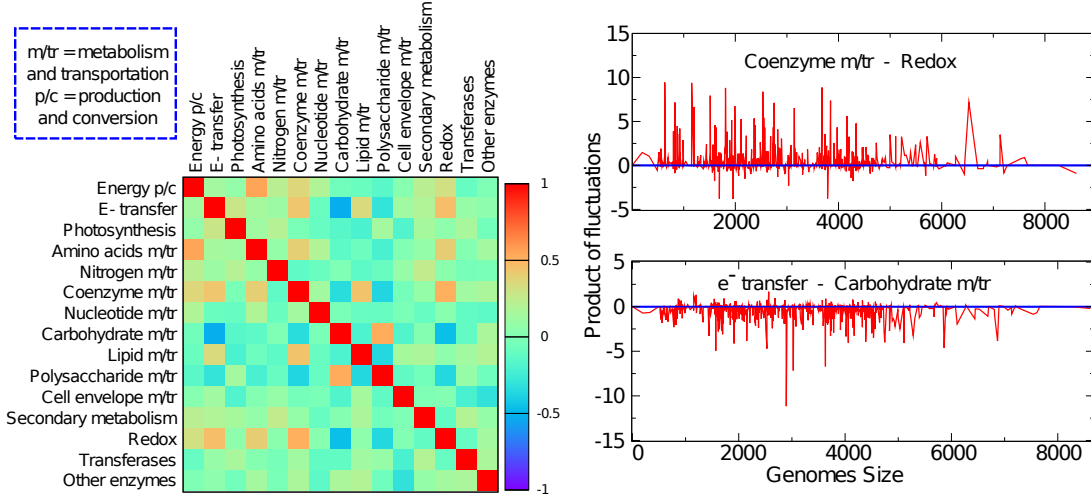


**Figure 6. Correlation between the populations of 24 different metabolic functional categories from the SUPERFAMILY database for 753 bacteria.** Left panel: Correlation matrix. Correlations are calculated from fluctuations of categories from the average trend (see Methods). Both correlation and anticorrelation are present between categories. Metabolism categories are highly (anti-)correlated. Right panel: product of fluctuations (in unit of variance) for two pairs of metabolic categories.

population of functional categories, we considered the correlation between the deviation of a family- or category population from the mean behavior at a given genome size  $n$  (Methods). The results are reported in Figure 6. The metabolism categories appear to be highly (anti-)correlated with each other, probably because of the role they play in different pathways of a common metabolic network [13]. The observed correlations between metabolic families might also be relevant for reproducing the correct tail of the family population histogram restricted to the metabolism category (Supplementary Figure S3).

An alternative approach is a description where the growth of each category is governed by intrinsic “evolutionary potentials” [3]. We have also analyzed such a description in some detail (see Supplementary text and Supplementary Figure S3). Despite of minor differences, a model with uncorrelated moves can also perform well in reproducing the joint scaling law and in predicting a relationship between the scaling exponents and the functional categories.

Figure 7 illustrates the basic differences between the two descriptions. The evolutionary potentials approach generically requires a lower number of parameters, but suffers from the tedious technical problem that the values of the growth coefficients cannot be controlled directly, because of the scaling of the normalization constant with genome size (Supplementary Text). The correlated model is technically more under control, since its behavior does not rely on any unknown normalization constant. For this reason, it also performs better with functional categories that grow faster than linear with genome size, such as transcription factors. Furthermore, such a model can be formulated with very few parameters once a synthetic description for the correlations, such as the toolbox model, is provided.

Overall, since functional categories scaling laws effectively emerge from the correlated approach, a good reconciliation of the two approaches could be to interpret the evolutionary potential model as an emergent description (which can be very useful in concrete empirical applications). In other words, evolutionary potentials would describe emergent effective growth of functional categories of a genome, averaging over more “microscopic” evolutionary processes where addition of genes belonging to specific functional categories needs to comply to constraints combining different functions to perform specific

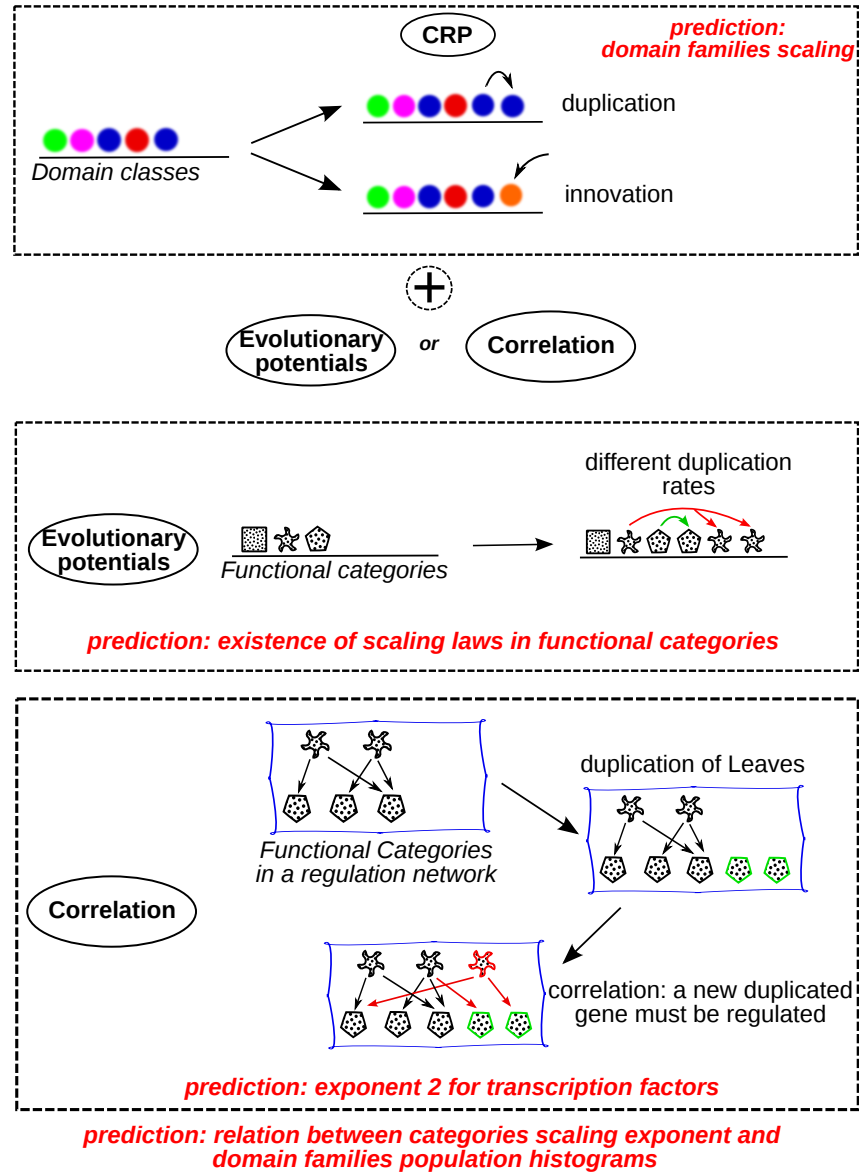


**Figure 7. Models with correlated versus absolute moves** Top: the Chinese restaurant process (CRP) acts on the homology families (colors) with a duplication and an innovation move. It is extended here to include functional categories (shapes) Middle: model with evolutionary potentials. Functional categories are assigned differential duplication rates as in ref [3]. Bottom: Model with correlated moves. Members of the functional categories are added proportionally between correlated pairs of functions (e.g. transcription factors and metabolic targets) as in ref. [13].

cell tasks. These kind of interactions between functions are better described by correlated growth of functional categories. In this view, genome growth would be governed by a relative recipe, where the proportions are more important than the exact amounts, rather than an absolute recipe, where only the detailed amounts of each ingredient play a role.

## Materials and Methods

### Data

Data on superfamily domain assignments and superfamily functional annotations for the 753 Bacteria were obtained from the SUPERFAMILY database [16]. The database contains 1291 different domain superfamilies grouped into 47 different functional categories (60 families do not belong to a specific category). These categories are divided into 6 larger groups (Metabolism, General, Regulation, Information, Initiation Complex Processes and Elongation Complex Processes, see also [http://supfam.cs.bris.ac.uk/SUPERFAMILY\\_1.73/function](http://supfam.cs.bris.ac.uk/SUPERFAMILY_1.73/function)).

### Models and Simulations

The quantitative duplication-innovation evolutionary models were explored by a mean-field analytical approach and direct numerical simulations. The mean-field approach considers equations for the means of the observed quantities in the large- $n$  approximation. In parallel with the mean-field analysis, we performed simulations of the main model and its variants. The realizations depend on the following parameters. (i) The parameters of a standard CRP,  $\alpha$  and  $\theta$ . (ii) The parameter  $\chi_c$ , i.e. the probability that a new family belongs to a given functional category. This parameter can be inferred from data. For example, for the case of transcription factors and targets, we defined  $\chi_{TF}$  from the slope extrapolated from Supplementary Figure S2, giving  $\chi_{TF} \simeq 0.035$  (see also Supplementary Figure S6). (iii) Initial conditions, represented by initial configuration (number of leaves, number of TFs and number of families in both categories). We have used the configuration of the smallest bacterium in the dataset (*Candidatus Carsonella ruddii*). An alternative choice could be the minimal intersection of all genomes in the database. (iv) Variant-specific parameters, that amount to the evolutionary potentials  $\rho_c$  for the first variant of the model, and the correlation matrix between functional categories,  $a_{ij}$  for the second variant. Simulation results are typically visualized in boxplots in order to compare the means with the probability distributions. In these plots bars correspond to (in order) the smallest observation, lower quartile, median, upper quartile, and largest observation.

### Empirical correlations among functional categories

Correlation between families (or categories) populations were calculated from the deviations from the average trend. We obtained the frequency of a family/category in every genome, defined as the ratio between the population of a family in domains and the total number of domains assigned on that genome. Subsequently for every family/category, we extracted an average trend as a function of genome size  $n$  using a sliding-window histogram (with window size of 280 domains and resolution of 28 domains), and we considered the deviation of each genome from the average trend at its value of  $n$ . The Pearson correlation of these deviations over all the genomes was considered between each pair of families/categories.

## References

1. Huynen MA, van Nimwegen E (1998) The frequency distribution of gene family sizes in complete genomes. *Mol Biol Evol* 15: 583-9.
2. van Nimwegen E (2003) Scaling laws in the functional content of genomes. *Trends in Genetics* 19: 479-484.
3. Molina N, van Nimwegen E (2008) The evolution of domain-content in bacterial genomes. *Biology Direct* : 51+.
4. Koonin EV, Wolf YI, Karev GP (2002) The structure of the protein universe and genome evolution. *Nature* 420: 218-23.
5. Dokholyan NV, Shakhnovich B, Shakhnovich EI (2002) Expanding protein universe and its origin from the biological Big Bang. *Proc Natl Acad Sci U S A* 99: 14132-6.
6. Cosentino Lagomarsino M, Sellerio A, Heijning P, Bassetti B (2009) Universal features in the genome-level evolution of protein domains. *Genome Biology* 10: R12+.
7. Perez-Rueda E, Janga S, Martinez-Antonio A (2009) Scaling relationship in the gene content of transcriptional machinery in bacteria. *Molecular Biosystems* .
8. Karev GP, Wolf YI, Rzhetsky AY, Berezovskaya FS, Koonin EV (2002) Birth and death of protein domains: a simple model of evolution explains power law behavior. *BMC Evol Biol* 2: 18.
9. Qian J, Luscombe NM, Gerstein M (2001) Protein family and fold occurrence in genomes: power-law behaviour and evolutionary model. *J Mol Biol* 313: 673-81.
10. Kamal M, Luscombe N, Qian J, Gerstein M (2006) Analytical Evolutionary Model for Protein Fold Occurrence in Genomes, Accounting for the Effects of Gene Duplication, Deletion, Acquisition and Selective Pressure. In: Koonin E, Wolf Y, Karev G, editors, *Power Laws, Scale-Free Networks and Genome Biology*, Springer, New York. pp. 165-193.
11. Durrett R, Schweinsberg J (2005) Power laws for family sizes in a duplication model. *Ann Probab* 33: 2094-2126.
12. Angelini A, Amato A, Bianconi G, Bassetti B, Lagomarsino MC (2009). Mean-field methods in duplication-innovation-loss models for the genomics of structural protein domains.
13. Maslov S, Krishna S, Pang T, Sneppen K (2009) Toolbox model of evolution of prokaryotic metabolic networks and their regulation. *Proceedings of the National Academy of Sciences* 106: 9743-9748.
14. Isambert H, Stein R (2009) On the need for widespread horizontal gene transfers under genome size constraint. *Biology Direct* 4: 28+.
15. Bornberg-Bauer E, Beaussart F, Kummerfeld SK, Teichmann SA, Weiner J 3rd (2005) The evolution of domain arrangements in proteins and interaction networks. *Cell Mol Life Sci* 62: 435-45.
16. Wilson D, Madera M, Vogel C, Chothia C, Gough J (2007) The superfamily database in 2007: families and function. *Nucleic Acids Res* : D308-D313.
17. Pitman J (2006) *Combinatorial Stochastic Process*. Notes for St. Flour Summer School. Berlin: Springer-Verlag.

18. Anantharaman V, Koonin EV, Aravind L (2001) Regulatory potential, phyletic distribution and evolution of ancient, intracellular small-molecule-binding domains. *J Mol Biol* 307: 1271–1292.
19. Chothia C, Gough J, Vogel C, Teichmann SA (2003) Evolution of the protein repertoire. *Science* 300: 1701–1703.
20. Charoensawan V, Wilson D, Teichmann SA (2010) Genomic repertoires of DNA-binding transcription factors across the tree of life. *Nucleic Acids Research* .
21. Koonin EV, Wolf YI (2008) Genomics of bacteria and archaea: the emerging dynamic view of the prokaryotic world. *Nucleic Acids Research* 36: 6688-6719.



## Supplementary Text and Figures for Grilli *et al.*

### S1 Model with evolutionary potentials.

This section introduces a variant of the model assigning evolutionary potentials [3]  $\rho_c$  to the functional categories, related to the probability that a gene added in a functional category is fixed by natural selection. Following the assumption that  $\rho_c$  act on family growth through the duplication move, the mean-field equations become

$$\partial_n n_i = p_O^i = \frac{\rho_{c(i)}(n_i - \alpha)}{\sum_{j=1}^F \rho_{c(j)} n_j + \theta}, \quad (3)$$

where  $\rho_{c(i)} = \rho_c$  if the homology family  $i$  belongs to the functional category  $c$ , and

$$\partial_n f = p_N = \frac{\alpha \sum_{j=1}^f \rho_{c(j)} + \theta}{\sum_{j=1}^f \rho_{c(j)} n_j + \theta}. \quad (4)$$

#### Evolutionary potentials can reproduce the combined scaling laws at finite sizes.

We tested this model variant by a combination of mean-field analytical arguments and direct simulation. Equations 3 and 4 guarantee that the system follows correct qualitative dynamics for the homology families. It is then necessary to verify that the population of the functional categories has the correct behaviour. The equation for the growth of the mean number of members  $n_c$  of a functional category can be obtained simply by summing on the homology families that belong to a given category. Using equations 3 and 4, and under the assumption (confirmed by empirical data, see Supplementary Figure S1) that the growth of old functional categories by adding new homology families through the innovation move is uniform (i.e. that  $f_c = \chi_c f$ ), we have the effective equation for large  $n$

$$\partial_n n_c = \frac{\rho_c n_c}{C(n)}, \quad (5)$$

where  $C(n) \simeq \sum_i \rho_i n_i$ . If  $C(n) \sim n$ , equation (5) corresponds to the evolution equation written by Molina and Nimwegen. Simulations of this model (see Supplementary Figure S7) confirm that this is the case. Thus, the mean-field prediction is that this model can reproduce both scaling laws.

Also note that a rescaling of  $C(n)$  is equivalent to a rescaling of  $\alpha$ . Indeed, for large  $n$ ,  $p_N \simeq \alpha F / C(n)$  (and  $p_O = 1 - p_N$ ), so imposing  $C(n) \simeq qn$  is equivalent to dividing  $\alpha$  by the constant factor  $q$ . Thus, one can choose  $q = 1$  without loss of generality (by a rescaling of all the  $\rho_c$ ), and the solution for the population of a functional category will be  $n_c(n) \sim n^{\rho_c/q}$  as in the Molina/Nimwegen model, then  $\zeta_c = \rho_c/q$ .

On the other hand, an important point regarding this model is that, asymptotically for any choice over the  $\rho_c$  set, the maximum large- $n$  exponent observed will be 1. Indeed, we can use the approximation  $C(n) = \sum_i \rho_i n_i \sim \rho_{\max} n^{\rho_c/q}$ , but  $C = qn$ , so that  $q = \rho_{c_{\max}}$ . This means that an exponent close to 2, such as that observed for transcription factors can only be obtained in a transient regime of the model. Furthermore, the change of the evolutionary potential of one functional category has repercussions on the other categories, as it implies a change in the normalization constant  $C$ . These facts make a direct identification of the value of the evolutionary potential with an intrinsic property of a single functional category difficult. They also make the direct identification of evolutionary potentials less straightforward (as it requires an arbitrary rescaling).

However, the above remarks have little practical importance, and the large- $n$  behaviour of the model does not really affect its performance at the relevant values of  $n$ . Numerical simulations show that at the empirical genome sizes, the scaling behaviour of the model can reproduce rather well the empirical one.

For simplicity we have restricted to three main categories (transcription factors, metabolic genes and “others”) and we verified that in practice it is not hard to find a parameter set in good agreement with the empirical data on protein domains (Supplementary Figure S3). The general number of parameters to adjust increases with the number of functional categories that one needs to consider.

## S2 Exponents of family size distribution histograms

This section discusses the family size distribution histograms, as obtained from the mean-field approach. It is possible to write a mean-field “flux equation” for the histograms [12], which implements the fact that each duplication adds a family with one extra member to the histogram count and subtracts a family with its previous population,

$$\partial_n f(d, n) = p_O(d-1, n)f(d-1, n) - p_O(d, n)f(d, n) + p_N \delta_{d,1}$$

where  $p_O(d, n) = \frac{j-\alpha}{n+\theta}$  is the probability that a family with  $d$  domains add a new duplicated member, and the source term contains the innovation probability  $p_N = \frac{\alpha f + \theta}{n + \theta}$  contributing to the growth of the number of families with one member. Note that the flow between families can be written as

$$\sum_{i \in \left\{ \substack{\text{families with} \\ j \text{ domains}} \right\}} \partial_n n_i = (d - \alpha) \frac{f(d, n)}{n + \theta}.$$

This equation requires an assumption on  $f(j, n)$  in order to be solved. Justified by simulation and empirical data [12] we assume  $f(j, n) = P(j)f(n)$ . Using the equation  $\partial_n f(n) = p_N$  gives the following equation for the probability of a family to have  $j$  members

$$\alpha P(d) = (d - 1 - \alpha)P(d) - (d - \alpha)P(j) ,$$

which can be easily solved in discrete or continuous  $d$  to get

$$P(d) \sim \left( \frac{1}{d} \right)^{1+\alpha} \quad (6)$$

predicting the asymptotic behaviour of data and simulations (see Figure 5) with  $\beta = \alpha$ .

In the correlated duplication model, the flux from transcription factor families caused by duplications is caused by two separate contribution, the CRP standard one, plus the TF duplications caused by duplications of any of the leaves

$$p_{O,TF}^i = \frac{1}{C(n)} \left[ (n_{i,TF} - \alpha) + \frac{n_{i,TF}}{n_L} (n_L - \alpha f_L) \right]$$

i.e.

$$p_{O,TF}^i = \frac{1}{C(n)} \left[ (n_{i,TF} \left( 2 - \frac{\alpha(1 - \chi_{TF})f}{n_L} \right) - \alpha) \right]$$

Thus, the flux equation for TF families becomes (for  $d > 1$ )

$$\begin{aligned} C(n) \partial_n f_{TF}(d, n) = & \left[ (d-1) \left( 2 - \frac{\alpha(1 - \chi_{TF})f}{n_L} \right) - \alpha \right] f_{TF}(d-1, n) \\ & - \left[ d \left( 2 - \frac{\alpha(1 - \chi_{TF})f}{n_L} \right) - \alpha \right] f_{TF}(d, n) \end{aligned}$$

We can solve this with the usual ansatz  $f_{TF}(d, n) = P_{TF}(d)f_{TF}(n)$ . Neglecting the subdominant term  $\frac{\alpha(1-\chi_{TF})f}{N_L}$  and using  $f_{TF}(n) = \chi_{TF}f(n)$ , leads to the equation

$$\alpha P_{TF}(d) = (2d - 2 - \alpha)P_{TF}(d) - (2d - \alpha)P_{TF}(d) , \quad (7)$$

which gives

$$P(d)_{TF} \sim \left(\frac{1}{d}\right)^{1+\frac{\alpha}{2}} , \quad (8)$$

that is  $\beta = \alpha/2 = \beta/2$ . In the above calculation we have supposed again that the number of TF domains are small with respect to the total number of leaf domains.

Furthermore, it can be argued that this fact is more general. Indeed, each time the per-family duplication probability for the TF functional category will have the form

$$p_O^i \simeq 2n_i ,$$

when family  $i$  belongs to TF category, the coefficient 2 will appear in the equation for  $P(d)_{TF}$  modifying the exponent. In particular, this will also be true for the model with evolutionary potentials.

In other words, each time a functional category scales with a given exponent, it can be argued on rather general grounds that the exponent of the population histograms of the homology families that form it will be affected. It is possible to generalize this argument, and find a precise relationship between the scaling exponent of a category and the family population histogram (restricted to the same category). In other words, if  $\zeta_c$  is the scaling exponent of the category  $c$  and  $\beta_c$  is the exponent of category family cumulative distribution histograms, that is (see equation 8):

$$P(d)_c \sim \left(\frac{1}{d}\right)^{1+\beta_c} ,$$

we suggest that  $\beta_c = \alpha/\zeta_c$ . We tested this prediction in empirical data plotting  $1/\beta_c$  versus  $\rho_c$  in Figure 5. The Pearson correlation coefficient in this is 0.47.

### S3 Comparison of model variants by numerical simulation

This section compares the correlated duplication and the evolutionary potential model variants. We considered a three categories model (TF, Metabolic and “other”).

The evolutionary potential model needs to supply three parameters  $\rho_c$ , while the correlated model needs to supply the correlation law between categories ( $a_{ij}$ ). We impose a correlation only between transcription factor and metabolic families with the toolbox model prescription, i.e.

$$a_{ij} = n_i/n_{met} , \quad (9)$$

where  $i$  is a TF family and  $j$  Metabolic,  $a_{ij} = 0$  (no correlation) otherwise.

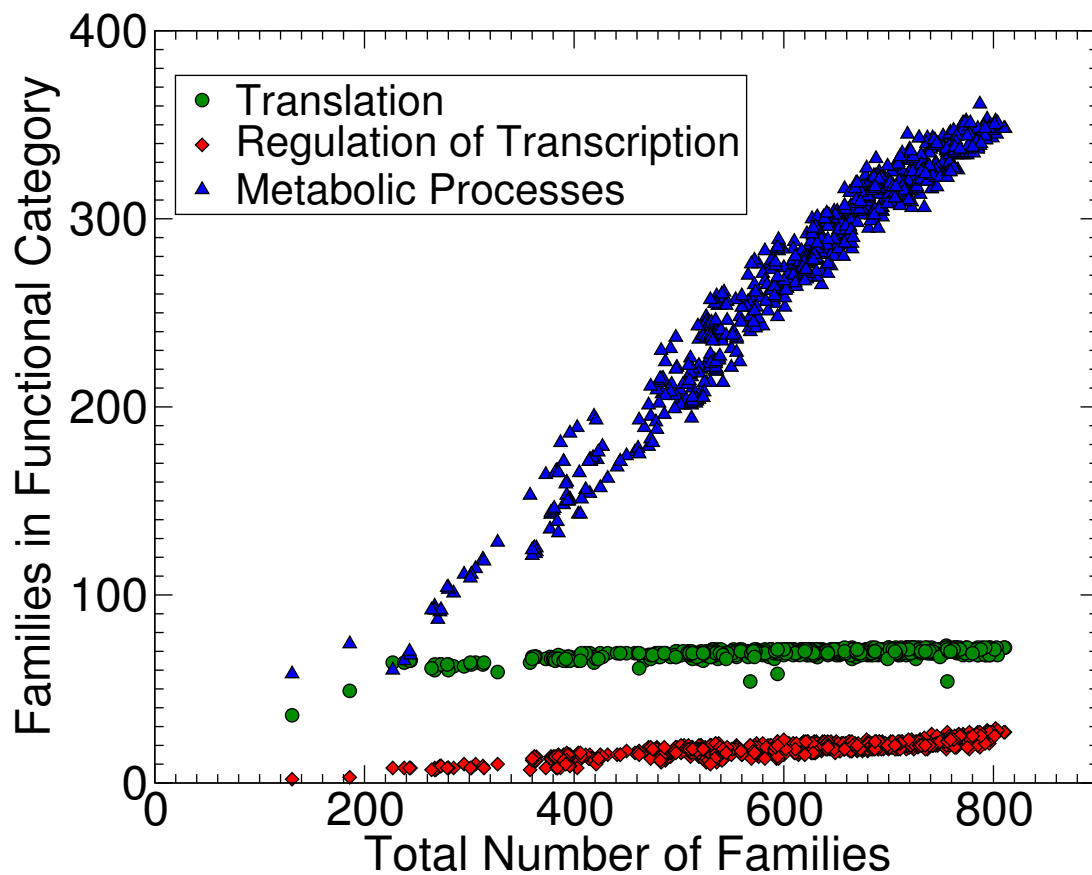
Figure S3 summarizes the results of this comparison. The correlated duplication model performs better in reproducing the behavior of the transcription factor category (both scaling law and histograms). Both models are unsatisfactory in reproducing the family population histogram of the metabolism families. This is probably caused by the fact that neither model include a correlation between metabolic families (Figure 6).

Figure S7 illustrates the behaviour of the normalization function  $C(n)$ .  $C(n)$  is linear with  $n$  in the range of empirical genome sizes (although the slope is not exactly 1). It becomes nonlinear at larger sizes, and its linear behavior is restored only at very large values of  $n$ .

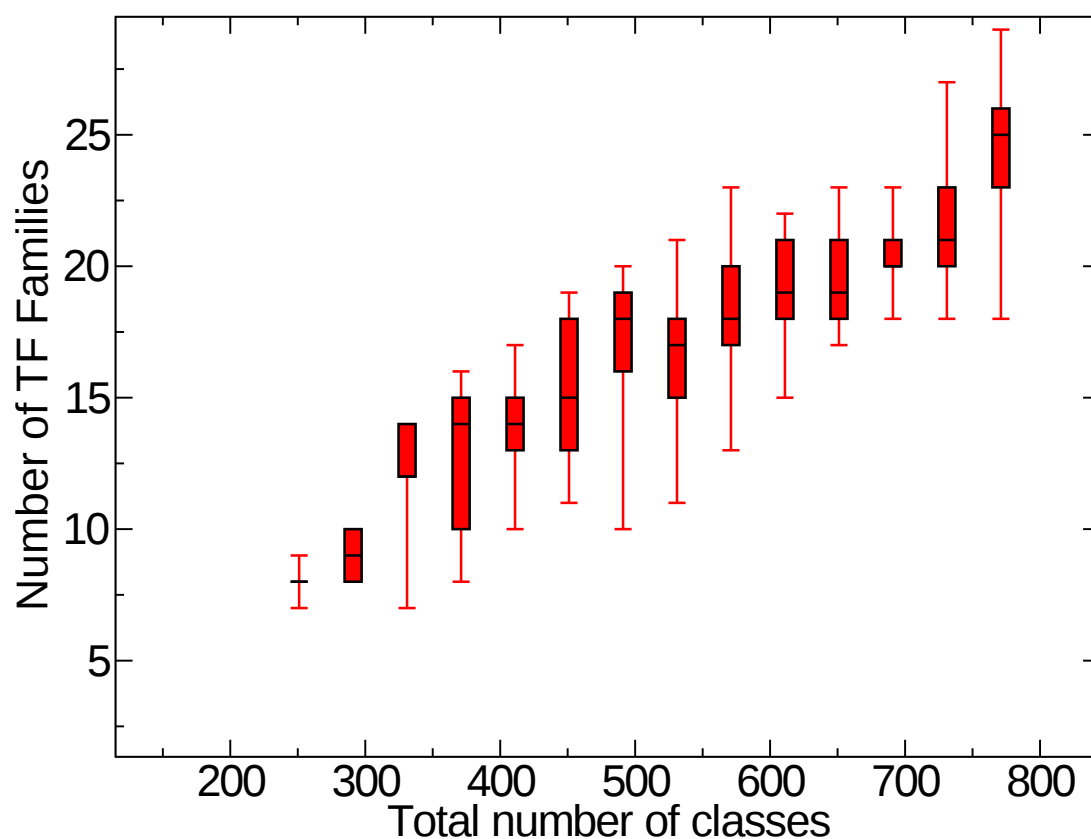
## S4 Details of TF-domain superfamily scaling

We observe that the TF quadratic (or very nearly so) scaling is clearly visible at in the two most populated families of transcription factor DNA-binding domains (Homeodomain-like and Winged-helix), which have a rather clean slope (see Supplementary Figure S4). In fact, three families present a clearly observable scaling alone (Homeodomain-like, Winged-helix and C-terminal), but just the first two follow a very nearly quadratic scaling.

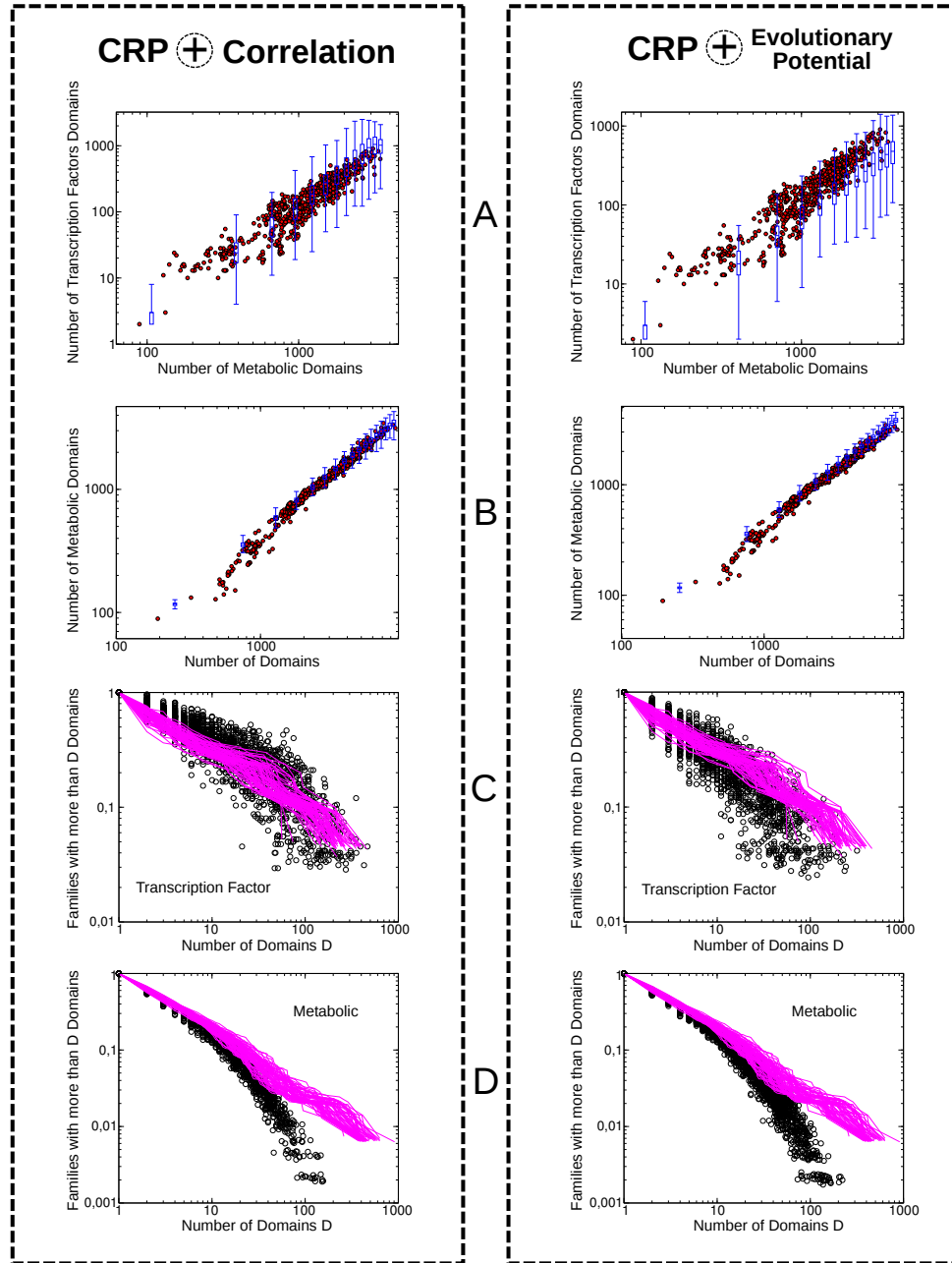
Note however that removing the six most populated TF families, representing 80% of the total TF-domain population, the remaining ones considered together still present a clear scaling when added up, but with exponent  $\simeq 1.12$ . This indicates that the collective scaling of TF families cannot be entirely recunducted to properties of the most populated ones, but these are the families responsible for the *quadratic* scaling.



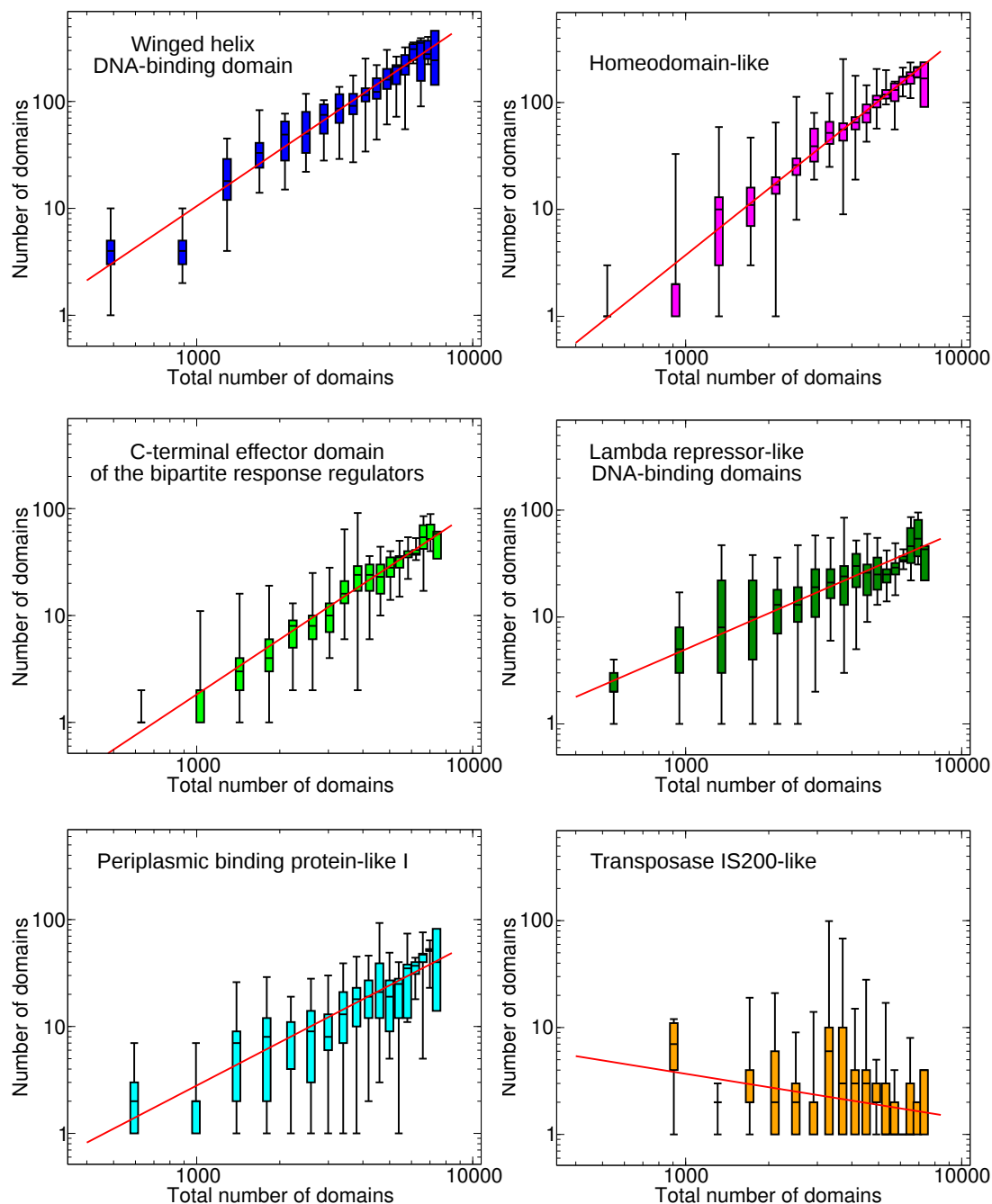
**Supplementary Figure S1. Linear scaling behaviour of the number of families in three important functional categories versus total number of families** from empirical data (for 753 bacteria in the SUPERFAMILY database). The slopes for the three linear laws are 0.01 (Translation), 0.03 (Regulation of Transcription) and 0.47 (Metabolic Processes).



**Supplementary Figure S2. Boxplot of the number of transcription factor domain families versus total number of domain families** (data from 753 SUPERFAMILY bacteria). There appears to be roughly linear scaling. This means that the number of TF domain families can be reproduced by a null hypothesis of independent addition model.

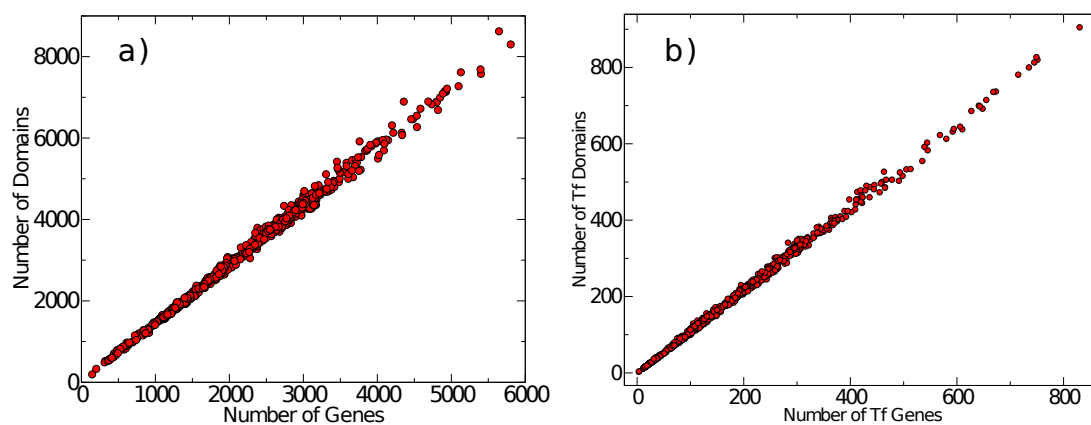


**Supplementary Figure S3. Comparison between simulation of the correlated duplication (left panel) and evolutionary potentials (right panel) model variants with empirical data.** Simulations are run at  $\alpha = 0.3$  and  $\theta 140$ . (a) Number of TFs domains vs. number of metabolic domains (the green boxplot corresponds to simulations, red circles to empirical data). (b) Number of metabolic domains vs. total numbers of domains (the green boxplot corresponds to simulations, red circles to empirical data). (c) Family population histograms restricted to the transcription factor functional category (black circles are simulations, magenta lines empirical data). (d) Family population histograms restricted to the metabolism functional category (black circles are simulations, magenta lines empirical data).

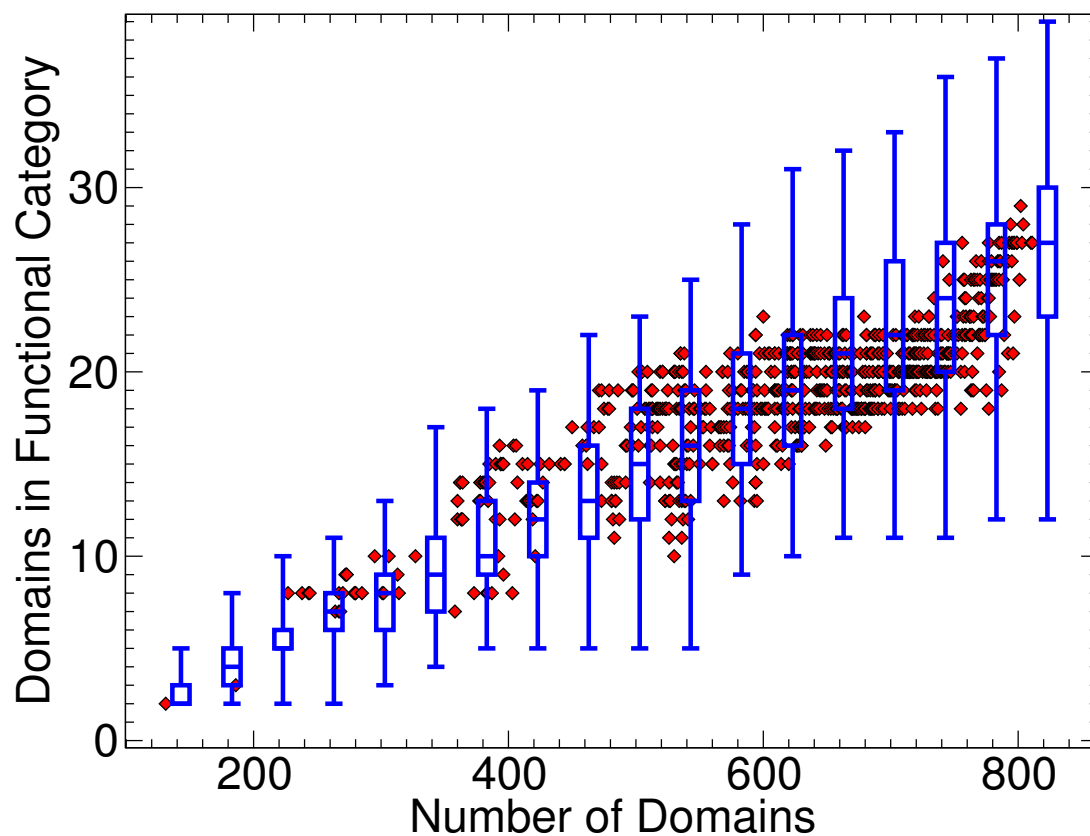


**Supplementary Figure S4. Boxplots for the population of the six most populated superfamilies of TF DNA-binding domains (y-axis in each panel) versus number of domains of each genome (x-axis in each panel).** The presence of scaling laws appears likely for the three most populated families and arguable for the first five. Red lines represent best power law fit (1.8 for Winged Helix ,2.1 for Homeodomain-like and 1.7 for C-terminal effector)

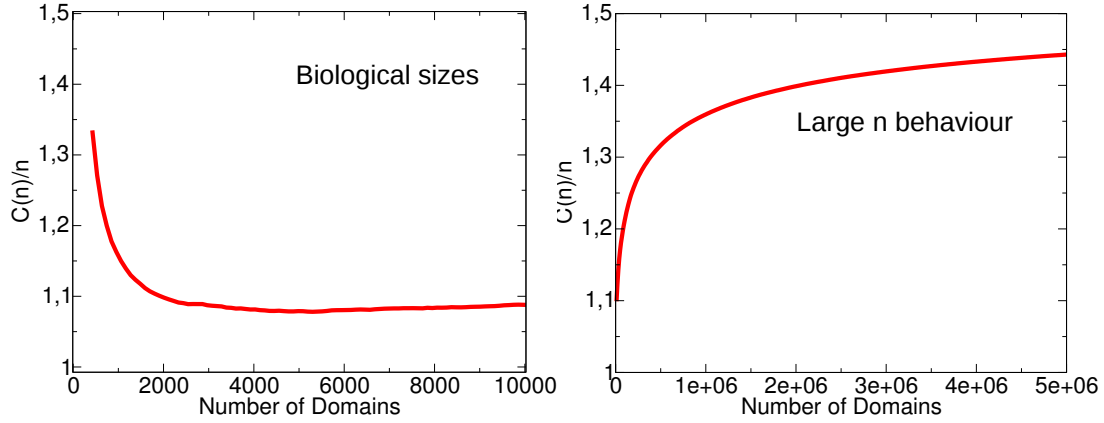




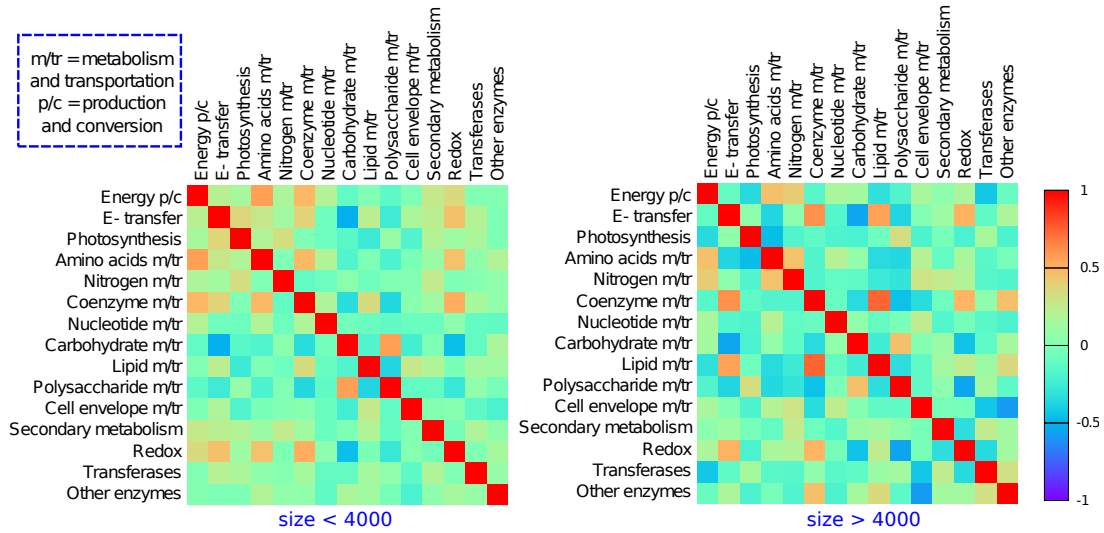
**Supplementary Figure S5. Linear relation between the number of domains and the number of genes** (a) Number of Domains vs. number of protein-coding genes for the 753 bacteria in the SUPERFAMILY database. There are, on average, 1.45 domains per gene. (b) Linear scaling behaviour of the number of TF domains vs. number of TF genes. There are, on average, 1.09 TF domains in a TF gene.



**Supplementary Figure S6. Comparison between empirical data and simulations of the number of TF domain families vs. total number of families.** The scaling is empirically linear: this means that the number of TF domain families can be reproduced by a null hypothesis of independent addition model. The choice of the parameter is 0.03.



**Supplementary Figure S7.** behavior of the ratio  $C(n)/n$ , where  $C(n)$  is the normalization factor for the evolutionary potential model. Data from simulations with three categories run at parameters  $\alpha = 0.3$  and  $\theta = 140$ .  $C(n)$  is linear with  $n$  in the range of empirical genome sizes, it then loses linearity, to become linear only asymptotically.



**Supplementary Figure S8.** Correlation matrix for two set of genomes with different sizes. Left side. Correlation Matrix for genomes with size < 4000. Right side. Correlation Matrix for genome with size > 4000. There are not a dependence on size of correlations.

Supplementary Table S1. Correlation coefficients between the populations of metabolic functional categories

	En	e-	Ph	Aa	N	Co	Nu	Ca	Li	Ps	Ce	2M	Rx	Tr	Ot
En	1	0.14	0.07	0.55	0.23	0.36	0.19	-0.06	-0.08	-0.14	0.02	0.22	0.31	-0.10	-0.004
e-	0.14	1	0.29	0.15	0.11	0.43	-0.09	-0.52	0.35	-0.29	0.13	0.19	0.47	0.09	0.05
Ph	0.07	0.29	1	0.12	0.21	-0.02	-0.09	-0.16	-0.21	0.14	-0.18	0.15	0.06	0.16	-0.05
Aa	0.55	0.15	0.12	1	0.08	0.39	0.19	-0.14	-0.07	-0.22	0.01	0.07	0.40	0.02	0.14
N	0.23	0.11	0.21	0.08	1	-0.13	-0.08	-0.003	-0.14	-0.09	0.09	0.26	0.04	-0.03	-0.02
Co	0.36	0.43	-0.02	0.39	-0.13	1	0.14	-0.33	0.44	-0.37	-0.04	0.08	0.51	0.12	0.16
Nu	0.19	-0.09	-0.09	0.19	-0.08	0.14	1	-0.03	-0.09	-0.10	-0.02	-0.10	0.03	-0.11	-0.13
Ca	-0.06	-0.52	-0.16	-0.14	-0.003	-0.33	-0.03	1	-0.20	0.53	-0.18	0.02	-0.46	-0.11	0.16
Li	-0.08	0.35	-0.21	-0.07	-0.14	0.44	-0.09	-0.20	1	-0.35	0.15	0.18	0.06	0.13	0.20
Ps	-0.14	-0.29	0.14	-0.22	-0.09	-0.37	-0.10	0.53	-0.35	1	-0.12	-0.05	-0.36	0.09	-0.07
Ce	0.02	0.13	-0.18	0.01	0.09	-0.04	-0.02	-0.18	0.15	-0.12	1	-0.0002	0.01	-0.22	-0.31
2M	0.22	0.19	0.15	0.07	0.26	0.08	-0.10	0.02	0.18	-0.05	-0.0002	1	-0.11	0.20	0.08
Rx	0.31	0.47	0.06	0.40	0.04	0.51	0.03	-0.46	0.06	-0.36	0.01	-0.11	1	-0.10	0.14
Tr	-0.10	0.09	0.16	0.02	-0.03	0.12	-0.11	-0.11	0.13	0.09	-0.22	0.20	-0.10	1	0.17
Ot	-0.004	0.05	-0.05	0.14	-0.02	0.16	-0.13	0.16	0.20	-0.07	-0.31	0.08	0.14	0.17	1

Pearson's correlation coefficients between the populations of 24 different metabolic functional categories from the SUPERFAMILY database for 753 bacteria. Correlations are calculated from fluctuations of categories from the average trend (see Methods). Both correlation and anticorrelation are present between categories. Metabolism categories are highly (anti-)correlated. We used the following short forms for the metabolic functional categories: En = Energy p/c, e- = Electrons transfer, Ph = Photosynthesis, Aa = Amino acids m/tr, N = Nitrogen m/tr, Co = Coenzyme m/tr, Nu = Nucleotide m/tr, Ca = Carbohydrate m/tr, Li = Lipid m/tr, Ps = Polysaccharide m/tr, Ce = Cell envelope m/tr, 2M = Secondary metabolism, Rx = Redox, Tr = Transferases, Ot = Other enzymes. Where m/tr stands for "metabolism and transportation" and p/c means "production and conversion".

Supplementary Table S2. P-Values of correlation coefficients between the populations of metabolic functional categories

	En	e-	Ph	Aa	N	Co	Nu	Ca	Li	Ps	Ce	2M	Rx	Tr	Ot
En	0	$5 \cdot 10^{-5}$	0.02	$< 10^{-6}$	$< 10^{-6}$	$< 10^{-6}$	$< 10^{-6}$	0.05	0.01	$4 \cdot 10^{-5}$	0.26	$< 10^{-6}$	$< 10^{-6}$	$4 \cdot 10^{-3}$	0.46
e-	$5 \cdot 10^{-5}$	0	$< 10^{-6}$	$2 \cdot 10^{-5}$	$1 \cdot 10^{-3}$	$< 10^{-6}$	$8 \cdot 10^{-3}$	$< 10^{-6}$	$< 10^{-6}$	$< 10^{-6}$	$3 \cdot 10^{-4}$	$1 \cdot 10^{-6}$	$< 10^{-6}$	$7 \cdot 10^{-3}$	0.08
Ph	0.02	$< 10^{-6}$	0	$1 \cdot 10^{-3}$	$< 10^{-6}$	0.29	$2 \cdot 10^{-3}$	$< 10^{-6}$	$< 10^{-6}$	$2 \cdot 10^{-4}$	$< 10^{-6}$	$5 \cdot 10^{-5}$	0.06	$2 \cdot 10^{-5}$	0.08
Aa	$< 10^{-6}$	$2 \cdot 10^{-5}$	$1 \cdot 10^{-3}$	0	0.02	$< 10^{-6}$	$2 \cdot 10^{-6}$	$4 \cdot 10^{-5}$	0.02	$< 10^{-6}$	0.39	0.03	$< 10^{-6}$	0.28	$5 \cdot 10^{-5}$
N	$< 10^{-6}$	$1 \cdot 10^{-3}$	$< 10^{-6}$	0.02	0	$2 \cdot 10^{-4}$	0.01	0.47	$7 \cdot 10^{-5}$	$5 \cdot 10^{-3}$	$8 \cdot 10^{-3}$	$< 10^{-6}$	0.13	0.18	0.31
Co	$< 10^{-6}$	$< 10^{-6}$	0.29	$< 10^{-6}$	$2 \cdot 10^{-4}$	0	$1 \cdot 10^{-4}$	$< 10^{-6}$	$< 10^{-6}$	$< 10^{-6}$	0.13	0.02	$< 10^{-6}$	$2 \cdot 10^{-4}$	$4 \cdot 10^{-6}$
Nu	$< 10^{-6}$	$8 \cdot 10^{-3}$	$2 \cdot 10^{-3}$	$2 \cdot 10^{-6}$	0.01	$1 \cdot 10^{-4}$	0	0.20	$5 \cdot 10^{-3}$	$3 \cdot 10^{-3}$	0.26	$3 \cdot 10^{-3}$	0.17	$8 \cdot 10^{-3}$	$9 \cdot 10^{-5}$
Ca	0.05	$< 10^{-6}$	$< 10^{-6}$	$4 \cdot 10^{-5}$	0.47	$< 10^{-6}$	0.20	0	$< 10^{-6}$	$< 10^{-6}$	$< 10^{-6}$	0.30	$< 10^{-6}$	$8 \cdot 10^{-4}$	$7 \cdot 10^{-6}$
Li	0.01	$< 10^{-6}$	$< 10^{-6}$	0.02	$7 \cdot 10^{-5}$	$< 10^{-6}$	$5 \cdot 10^{-3}$	$< 10^{-6}$	0	$< 10^{-6}$	$3 \cdot 10^{-5}$	$< 10^{-6}$	0.06	$3 \cdot 10^{-4}$	$2 \cdot 10^{-6}$
Ps	$4 \cdot 10^{-5}$	$< 10^{-6}$	$2 \cdot 10^{-4}$	$< 10^{-6}$	$5 \cdot 10^{-3}$	$< 10^{-6}$	$3 \cdot 10^{-3}$	$< 10^{-6}$	$< 10^{-6}$	0	$5 \cdot 10^{-4}$	0.07	$< 10^{-6}$	$6 \cdot 10^{-3}$	0.03
Ce	0.26	$3 \cdot 10^{-4}$	$< 10^{-6}$	0.39	$8 \cdot 10^{-3}$	0.13	0.26	$< 10^{-6}$	$3 \cdot 10^{-5}$	$5 \cdot 10^{-4}$	0	0.50	0.38	$< 10^{-6}$	$< 10^{-6}$
2M	$< 10^{-6}$	$1 \cdot 10^{-6}$	$5 \cdot 10^{-5}$	0.03	$< 10^{-6}$	0.02	$3 \cdot 10^{-3}$	0.30	$< 10^{-6}$	0.07	0.50	0	$8 \cdot 10^{-4}$	$< 10^{-6}$	0.01
Rx	$< 10^{-6}$	$< 10^{-6}$	0.06	$< 10^{-6}$	0.13	$< 10^{-6}$	0.17	$< 10^{-6}$	0.06	$< 10^{-6}$	0.38	$8 \cdot 10^{-4}$	0	$3 \cdot 10^{-3}$	$4 \cdot 10^{-5}$
Tr	$4 \cdot 10^{-3}$	$7 \cdot 10^{-3}$	$2 \cdot 10^{-5}$	0.28	0.18	$2 \cdot 10^{-4}$	$8 \cdot 10^{-4}$	$8 \cdot 10^{-4}$	$3 \cdot 10^{-4}$	$6 \cdot 10^{-3}$	$< 10^{-6}$	$< 10^{-6}$	$3 \cdot 10^{-3}$	0	$1 \cdot 10^{-6}$
Ot	0.46	0.08	0.08	$5 \cdot 10^{-5}$	0.31	$4 \cdot 10^{-6}$	$9 \cdot 10^{-5}$	$7 \cdot 10^{-6}$	$2 \cdot 10^{-6}$	0.03	$< 10^{-6}$	0.01	$4 \cdot 10^{-5}$	$1 \cdot 10^{-6}$	0

P-values of the Pearson's correlation coefficients between the populations of 24 different metabolic functional categories from the SUPERFAMILY database for 753 bacteria. Correlations are calculated from fluctuations of categories from the average trend (see Methods). The (anti-)correlation is statistically significant for the most of the metabolic categories. We used the following short forms for the metabolic functional categories: En = Energy p/c, e- = Electrons transfer, Ph = Photosynthesis, Aa = Amino acids m/tr, N = Nitrogen m/tr, Co = Coenzyme m/tr, Nu = Nucleotide m/tr, Ca = Carbohydrate m/tr, Li = Lipid m/tr, Ps = Polysaccharide m/tr, Ce = Cell envelope m/tr, 2M = Secondary metabolism, Rx = Redox, Tr = Transferases, Ot = Other enzymes. Where m/tr stands for "metabolism and trasportation" and p/c means "production and conversion".